

Supporting Information for

The layered RuBr₃-RuI₃ honeycomb system

Danrui Ni, Xianghan Xu, Robert J. Cava*

Department of Chemistry, Princeton University, Princeton, NJ 08544, USA

*E-mail: rcava@princeton.edu

This SI includes:

- CCDC deposition numbers for α -Ru(Br_{1-x}I_x)₃ structures.
- Table S1. Single-crystal crystallographic data of α -Ru(Br_{1-x}I_x)₃.
- Table S2. Selected bond lengths and bond angles of α -Ru(Br_{1-x}I_x)₃.
- Figure S1. Representative PXRD patterns with Le Bail fittings.
- Figure S2. PXRD and magnetic susceptibility data of β -RuBr₂I.
- Figure S3. Magnetic susceptibility data of α -Ru(Br_{1-x}I_x)₃ ($x = 0, 0.25, 0.5$).
- Figure S4. The total heat capacity versus temperature of α -Ru(Br_{1-x}I_x)₃ from 2 to 150 K.
- Figure S5. The field-dependent magnetization of α -Ru(Br_{1-x}I_x)₃ at 250 K.
- Figure S6. The selected field-dependent magnetization α -Ru(Br_{1-x}I_x)₃ at 2 K.
- Figure S7. Resistivity ρ_0 at 275 K of α -Ru(Br_{1-x}I_x)₃ samples.
- Figure S8. Representative plots of $\ln(\rho)$ vs $1/T$ fittings of α -Ru(Br_{1-x}I_x)₃.

Supplementary Text

CCDC deposition number of refined crystal structure

CCDC number 2299103-2299108 contains the supplemental crystallographic data for this paper. These data can be obtained free of charge (available at www.ccdc.cam.ac.uk/data_request/cif, or by emailing data_request@ccdc.cam.ac.uk, or by contacting The Cambridge Crystallographic Data Centre, 12 Union Road, Cambridge CB2 1EZ, UK, fax: + 441223336033).

Table S1. Crystal Data and Structure Refinements for α -Ru(Br,I)₃ at 300 K. Standard deviations in temperature and cell parameters are indicated by the values in parentheses.

Refined Formula	Ru _{0.924} Br _{0.5} I _{2.5}	Ru _{1.009} Br _{0.75} I _{2.25}	Ru _{0.923} BrI ₂	Ru _{0.937} Br _{1.5} I _{1.5}	Ru _{0.957} Br ₂ I	Ru _{0.960} Br _{2.25} I _{0.75}
Temperature (K)	295(2)	287(2)	300(2)	300(2)	300 (2)	300 (2)
F.W. (g/mol)	450.69	446.52	426.90	404.34	383.44	371.99
Crystal System	Trigonal	Trigonal	Trigonal	Trigonal	Trigonal	Trigonal
Space Group	<i>R</i> -3 (148)	<i>R</i> -3 (148)	<i>R</i> -3 (148)	<i>R</i> -3 (148)	<i>R</i> -3 (148)	<i>R</i> -3 (148)
Unit Cell Dimension <i>a</i> (Å)	6.7749(8)	6.7413(11)	6.7210(9)	6.6379(6)	6.5237(3)	6.458(3)
Unit Cell Dimension <i>c</i> (Å)	18.990(3)	18.993(4)	19.026(4)	18.947(3)	18.7106(15)	18.541(12)
Volume (Å ³)	754.8(2)	747.5(3)	744.3(2)	722.99(16)	689.61(8)	669.7(7)
Z	6	6	6	6	6	6
Calculated Density (g/cm ³)	5.949	5.952	5.714	5.572	5.540	5.534
Absorption Coefficient (mm ⁻¹)	22.012	22.902	23.229	24.884	27.157	28.481
F(000)	1144	1137	1089	1038	991	964
Theta range for data collection	3.218° to 24.722°	3.218° to 24.695°	3.212° to 24.692°	3.226° to 25.359°	3.266° to 24.501°	3.296° to 24.744°
Index Ranges	-7 ≤ <i>h</i> ≤ 7, -7 ≤ <i>k</i> ≤ 7, -22 ≤ <i>l</i> ≤ 22	-7 ≤ <i>h</i> ≤ 7, -7 ≤ <i>k</i> ≤ 7, -22 ≤ <i>l</i> ≤ 22	-7 ≤ <i>h</i> ≤ 7, -7 ≤ <i>k</i> ≤ 7, -22 ≤ <i>l</i> ≤ 22	-7 ≤ <i>h</i> ≤ 7, -7 ≤ <i>k</i> ≤ 7, -22 ≤ <i>l</i> ≤ 22	-7 ≤ <i>h</i> ≤ 7, -7 ≤ <i>k</i> ≤ 7, -21 ≤ <i>l</i> ≤ 21	-7 ≤ <i>h</i> ≤ 7, -7 ≤ <i>k</i> ≤ 7, -21 ≤ <i>l</i> ≤ 21
Reflections Collected	4480	4415	2733	4354	3356	2092
Independent Reflections	290 [R(int) = 0.0335]	287 [R(int) = 0.0675]	289 [R(int) = 0.0538]	294 [R(int) = 0.0423]	270 [R(int) = 0.0502]	268 [R(int) = 0.1746]
Goodness-of-fit on F ²	1.204	1.152	1.144	1.152	1.164	1.131
Final R Indices [<i>I</i> > σ(<i>I</i>)]	R1 = 0.0271, wR2 = 0.0636	R1 = 0.0447, wR2 = 0.1241	R1 = 0.0498, wR2 = 0.1103	R1 = 0.0237, wR2 = 0.0604	R1 = 0.0285, wR2 = 0.0646	R1 = 0.1041, wR2 = 0.1310
R Indices (all data)	R1 = 0.0307, wR2 = 0.0656	R1 = 0.0491, wR2 = 0.1293	R1 = 0.0591, wR2 = 0.1144	R1 = 0.0367, wR2 = 0.0721	R1 = 0.0411, wR2 = 0.0681	R1 = 0.1654, wR2 = 0.1489
Largest Diff. Peak and Hole (e.Å ⁻³)	1.300 and -1.190	2.026 and -2.155	2.456 and -1.222	1.063 and -1.636	1.200 and -1.403	1.534 and -1.912

Table S2. Selected bond lengths (Å) and bond angles (°) for α -Ru(Br,I)₃ at 300 K. X represents the atom on the 18f site which is occupied in a disordered fashion by Br and I. Standard deviation is indicated by the values in parentheses.

	Ru_{0.924}Br_{0.5}I_{2.5}		Ru_{1.009}Br_{0.75}I_{2.25}		Ru_{0.923}BrI₂	
Bond Length (Å)	Ru1-X (x3)	2.6821(10)	Ru1-X (x3)	2.6594(12)	Ru1-X (x3)	2.6537(19)
	Ru1-X (x3)	2.6898(10)	Ru1-X (x3)	2.6654(11)	Ru1-X (x3)	2.6615(19)
	Ru2-X (x6)	2.7842(6)	Ru2-X (x6)	2.7975(11)	Ru2-X (x6)	2.7926(12)
Bond Angle (°)	X-Ru1-X (x3)	91.55(4)	X-Ru1-X (x3)	91.89(4)	X-Ru1-X (x3)	92.04(5)
	X-Ru1-X (x3)	91.25(4)	X-Ru1-X (x3)	91.35(5)	X-Ru1-X (x3)	91.18(8)
	X-Ru1-X (x3)	90.73(3)	X-Ru1-X (x3)	90.83(5)	X-Ru1-X (x3)	90.70(8)
	X-Ru1-X (x3)	86.54(2)	X-Ru1-X (x3)	86.07(3)	X-Ru1-X (x3)	86.22(4)
	X-Ru1-X (x3)	177.06(2)	X-Ru1-X (x3)	175.90(4)	X-Ru1-X (x2)	175.90(5)
				X-Ru1-X (x1)	175.89(5)	
	Ru_{0.937}Br_{1.5}I_{1.5}		Ru_{0.957}Br₂I		Ru_{0.960}Br_{2.25}I_{0.75}	
Bond Length (Å)	Ru1-X (x3)	2.6301(8)	Ru1-X (x3)	2.5872(9)	Ru1-X (x3)	2.554(5)
	Ru1-X (x3)	2.6363(8)	Ru1-X (x3)	2.5910(9)	Ru1-X (x3)	2.568(5)
	Ru2-X (x6)	2.7501(6)	Ru2-X (x6)	2.7101(7)		
Bond Angle (°)	X-Ru1-X (x3)	91.70(3)	X-Ru1-X (x3)	92.02(3)	X-Ru1-X (x3)	92.14(14)
	X-Ru1-X (x3)	91.10(3)	X-Ru1-X (x3)	90.97(3)	X-Ru1-X (x6)	90.7(2)
	X-Ru1-X (x3)	90.70(3)	X-Ru1-X (x3)	90.46(4)	X-Ru1-X (x3)	86.57(10)
	X-Ru1-X (x3)	86.61(2)	X-Ru1-X (x3)	86.67(2)	X-Ru1-X (x2)	176.09(13)
	X-Ru1-X (x3)	176.42(2)	X-Ru1-X (x2)	176.21(3)	X-Ru1-X (x1)	176.08(13)
		X-Ru1-X (x1)	176.22(3)			

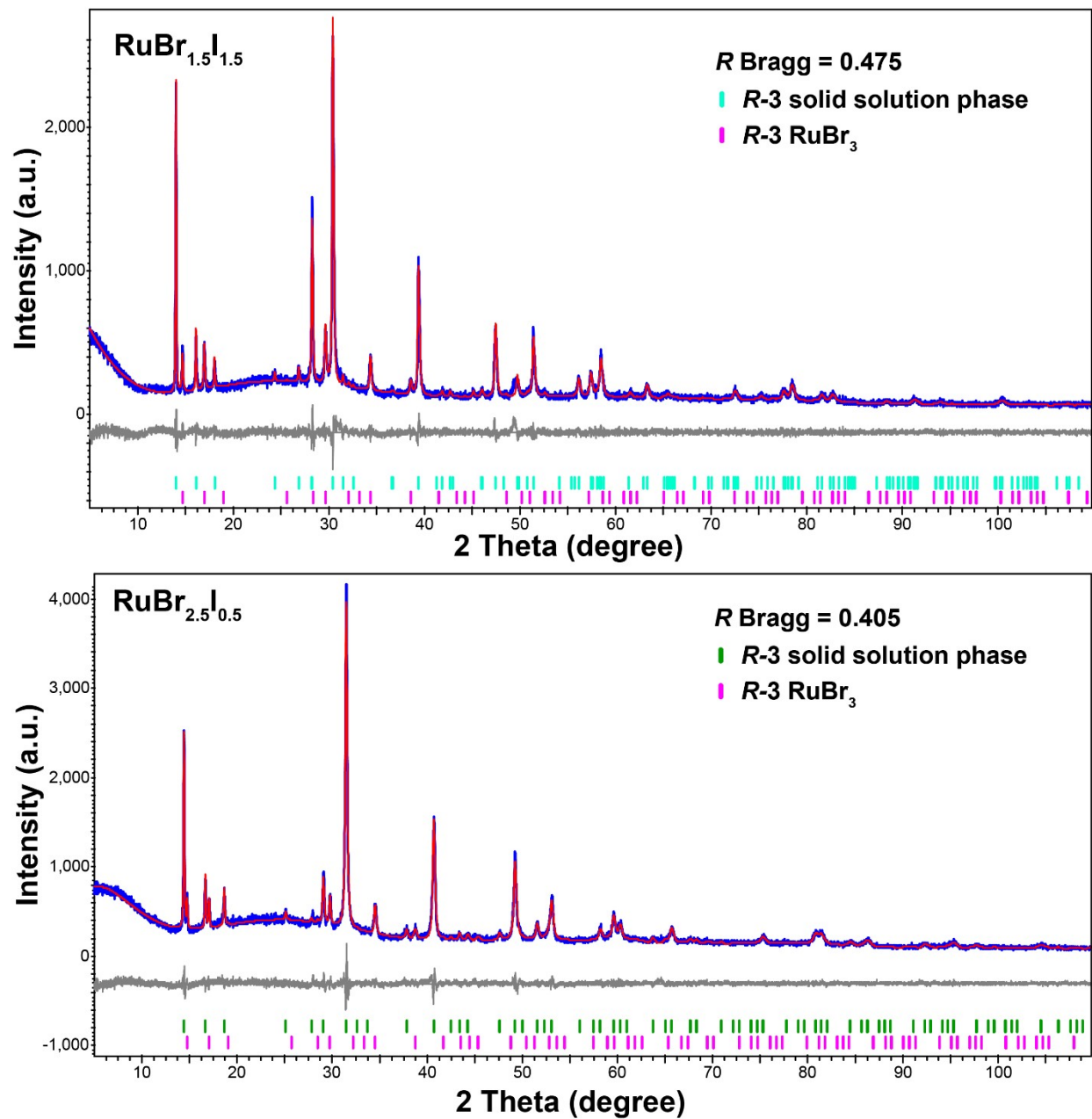


Figure S1. Representative PXR D patterns with Le Bail fit for bulk α -Ru(Br_{1-x}I_x)₃ materials (top $x = 0.5$, bottom $x = 0.17$), confirming the consistency of the bulk sample structure and composition with the SCXRD refinement results.

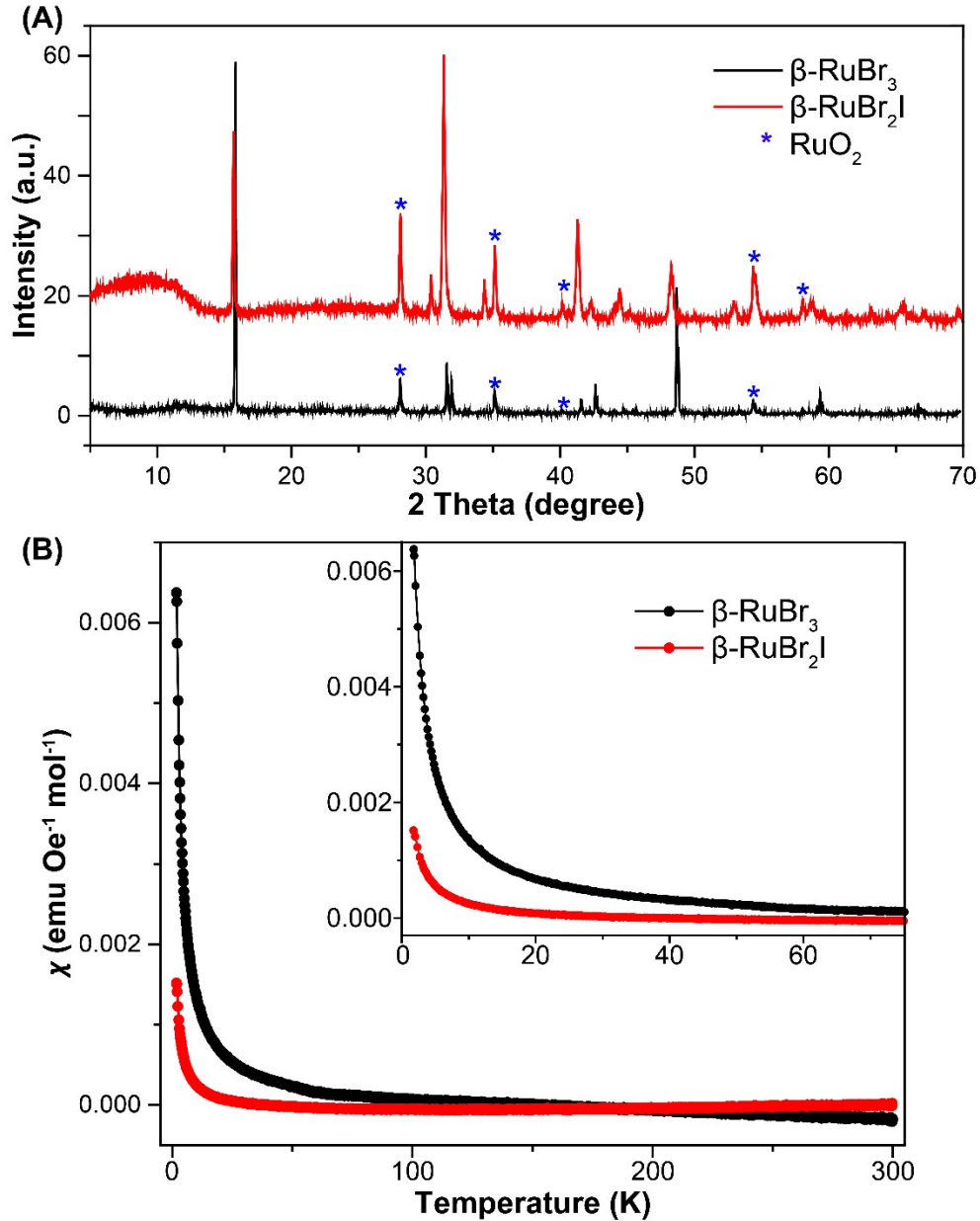


Figure S2. (A) PXRD patterns of undoped 1D-chain structure β -RuBr₃ (black pattern), and isostructural β -RuBr₂I (red pattern) synthesized at ambient pressure (annealed at 400 – 600 °C under vacuum in sealed quartz tube for five days). RuO₂ impurity phase is labeled with * in the pattern. Comparing the two patterns, the shift of peaks with similar diffraction type suggests the iodine successfully doped into the 1D chain lattice without changing the structure. (B) Temperature dependent magnetic susceptibility (χ) of β -RuBr₃ and β -RuBr₂I, measured under 1000 Oe (ZFC) from 1.8 to 300 K. The inset shows a zoomed-in view of the 1.8 to 75 K range, confirming that no 3D magnetic ordering or transitions can be observed in the low temperature range for both samples.

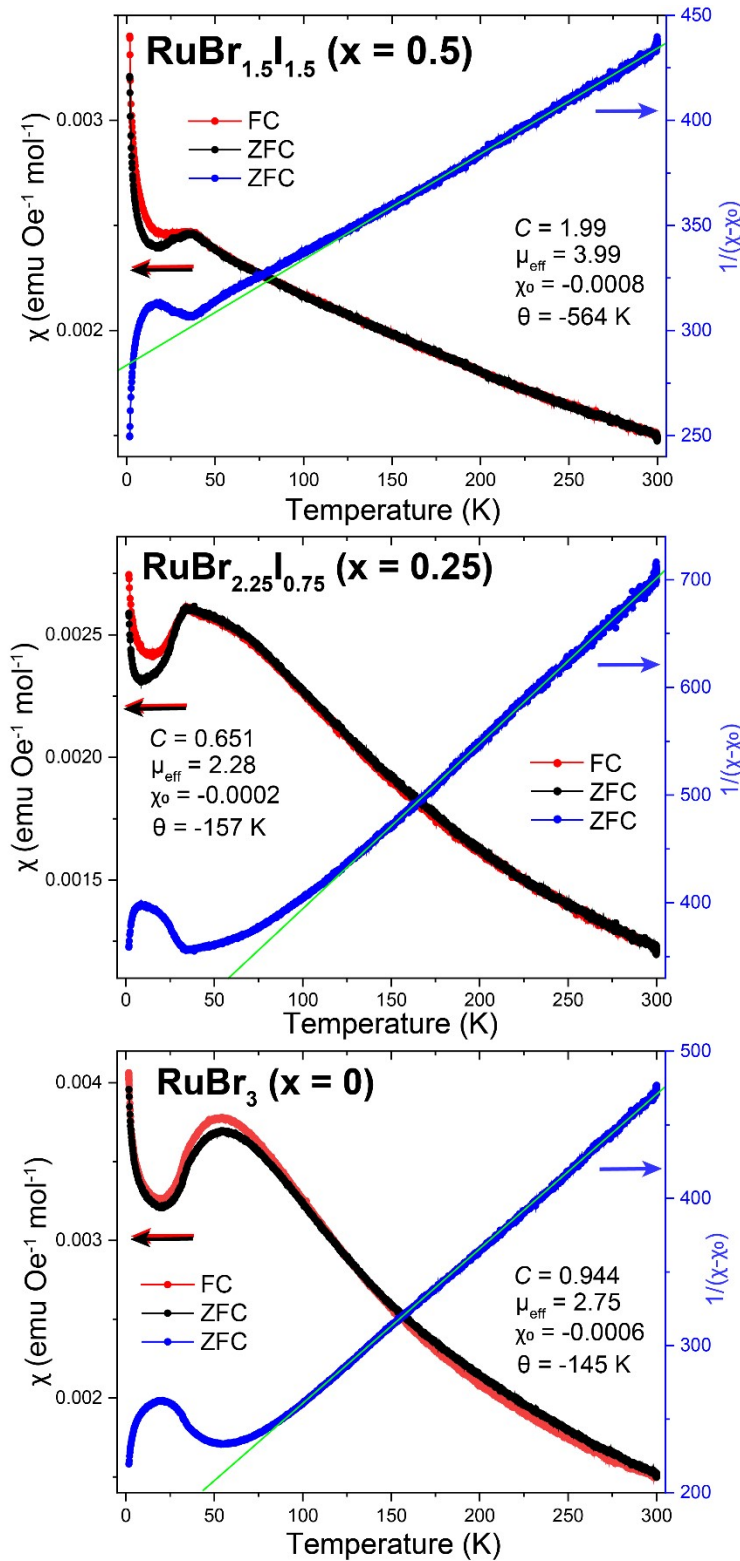


Figure S3. The χ vs. T plots of honeycomb-structure $\alpha\text{-Ru}(\text{Br}_{1-x}\text{I}_x)_3$ (ZFC in black and FC in red), with the $1/(\chi - \chi_0)$ vs. T curves in blue color. Curie-Weiss fitting is conducted and the parameters are labeled in the panel. Top $x = 0.5$, middle $x = 0.25$, bottom $x = 0$.

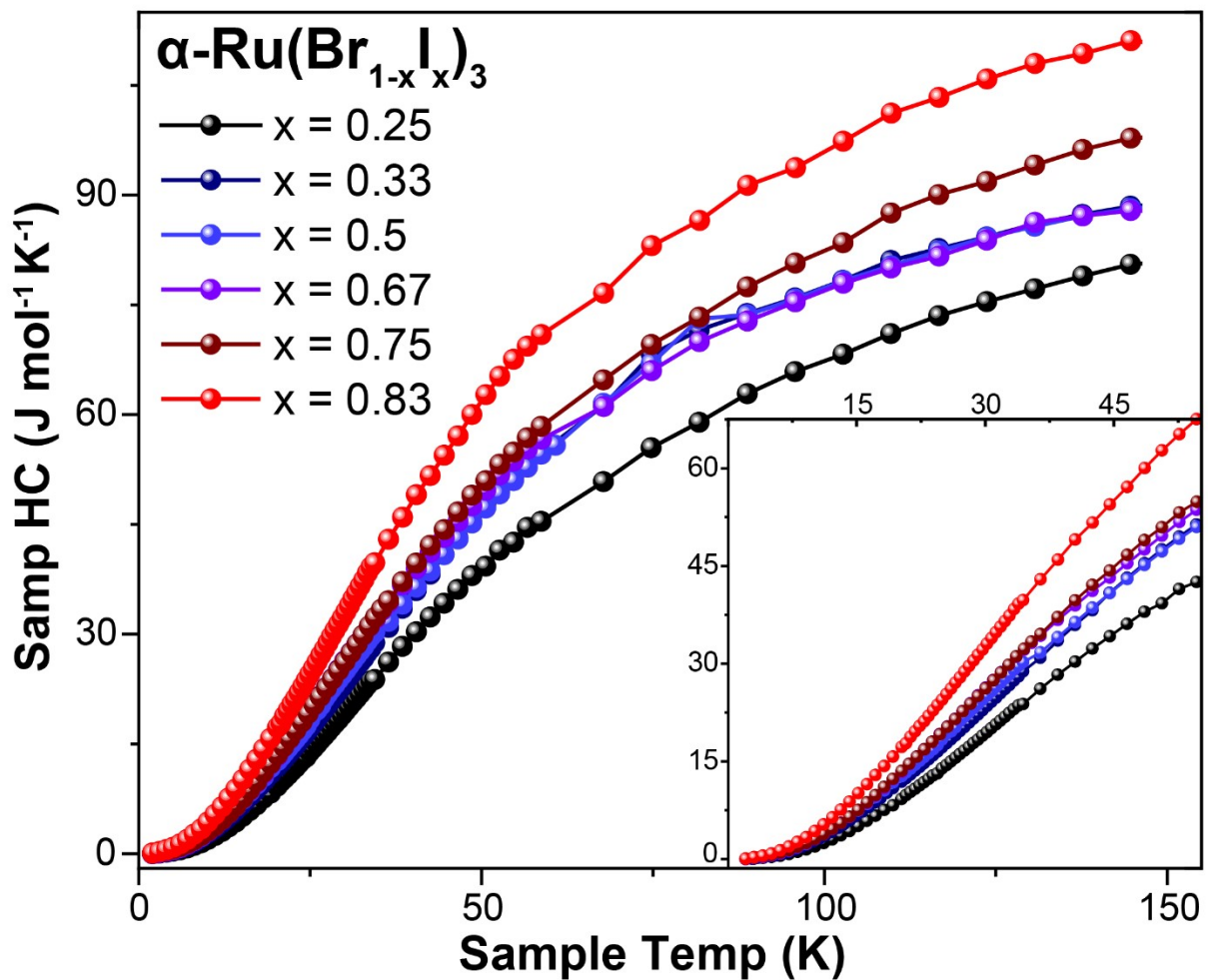


Figure S4. The total heat capacity (HC) versus temperature of $\alpha\text{-Ru}(\text{Br}_{1-x}\text{I}_x)_3$ from 2 to 150 K, with the 2 to 50 K range enlarged in the inset. The total atomic number is fixed to 4 to correct the errors that may be introduced by the samples' weights.

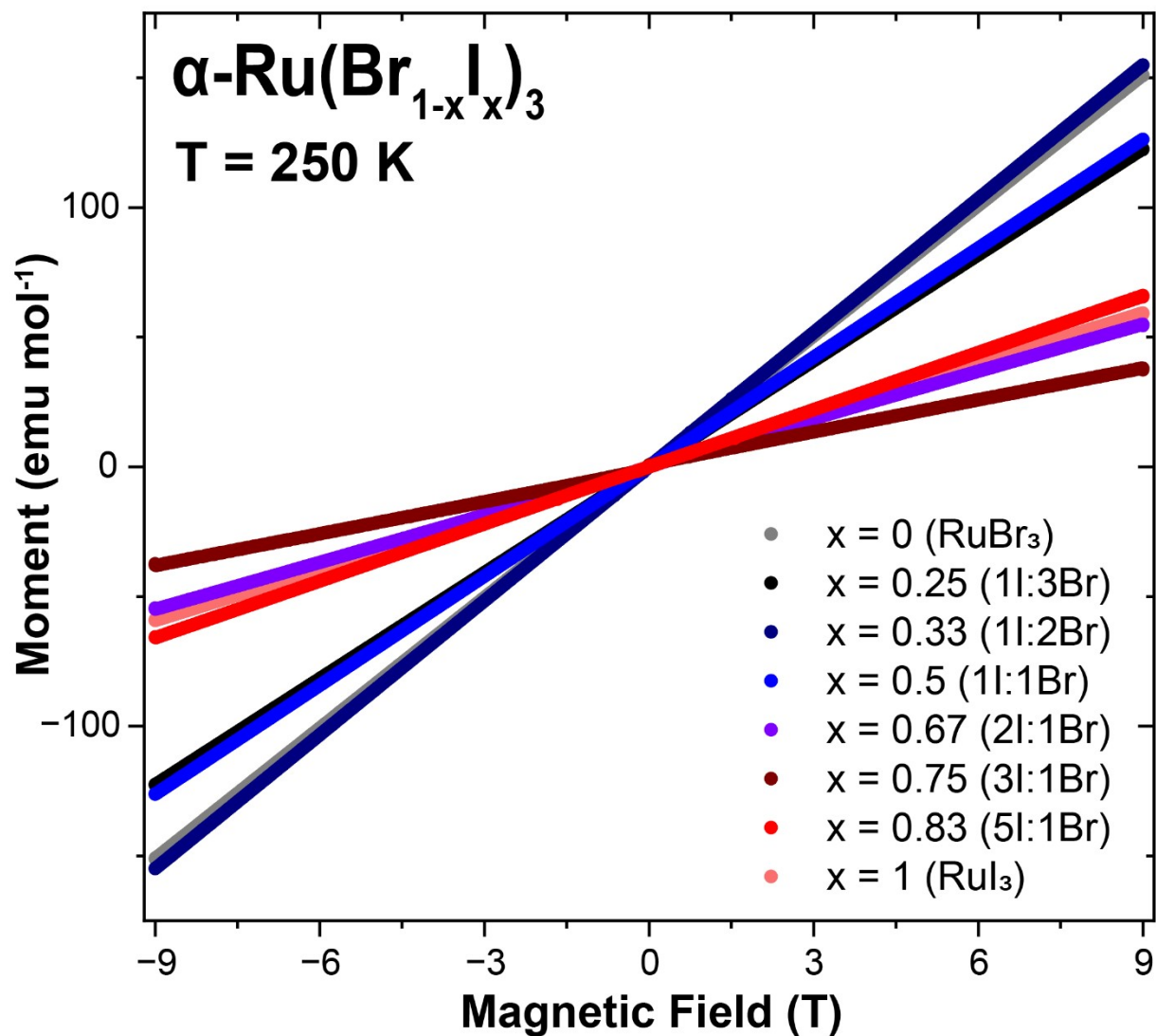


Figure S5. The field-dependent magnetization data collected at 250 K of honeycomb-structure $\alpha\text{-Ru}(\text{Br}_{1-x}\text{I}_x)_3$ ($0 \leq x \leq 1$).

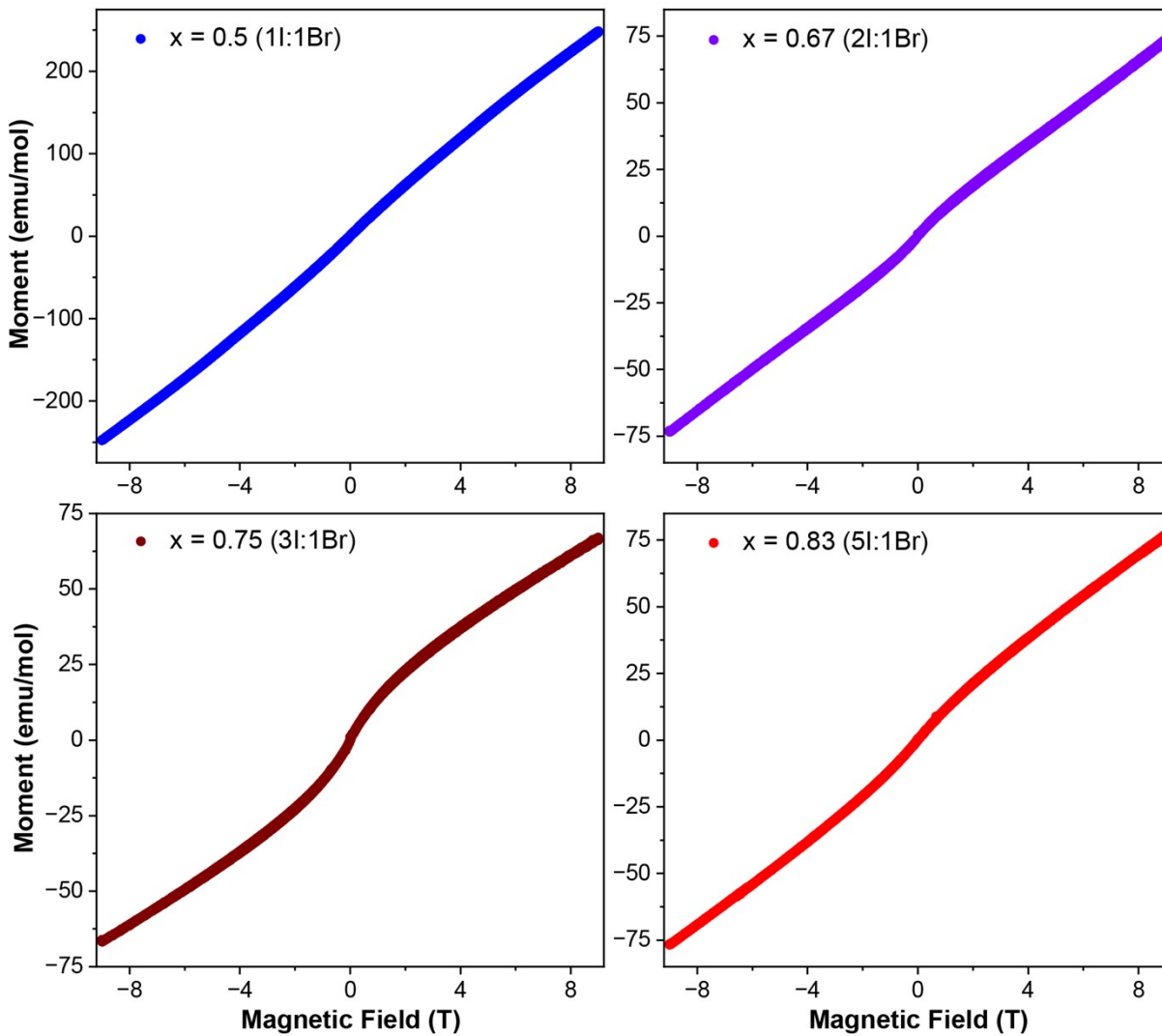


Figure S6. The selected field-dependent magnetization data collected at 2 K of $\alpha\text{-Ru}(\text{Br}_{1-x}\text{I}_x)_3$ with $x = 0.5, 0.67, 0.75,$ and 0.83 .

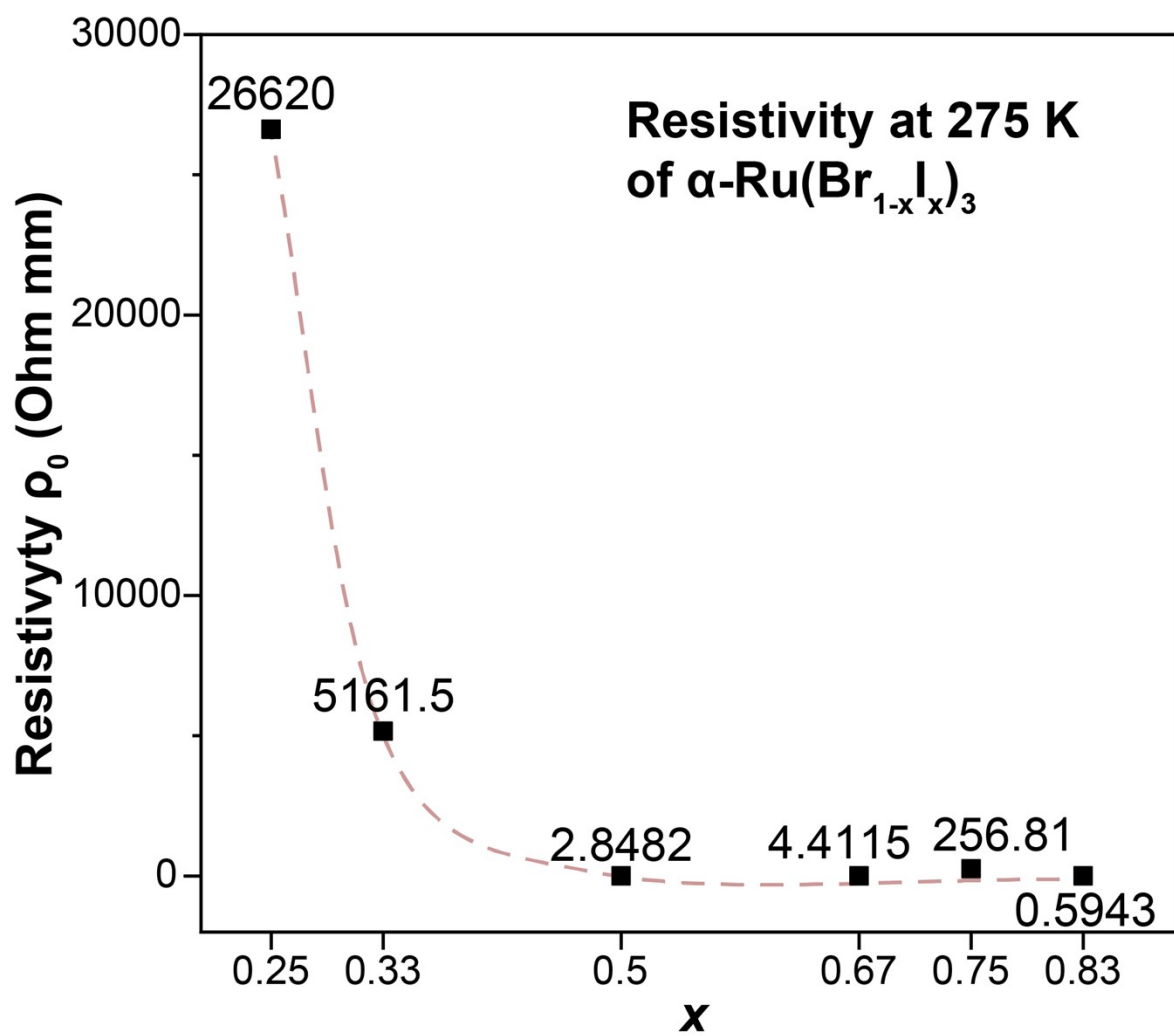


Figure S7. Resistivity ρ_0 at 275 K of $\alpha\text{-Ru}(\text{Br}_{1-x}\text{I}_x)_3$ samples.

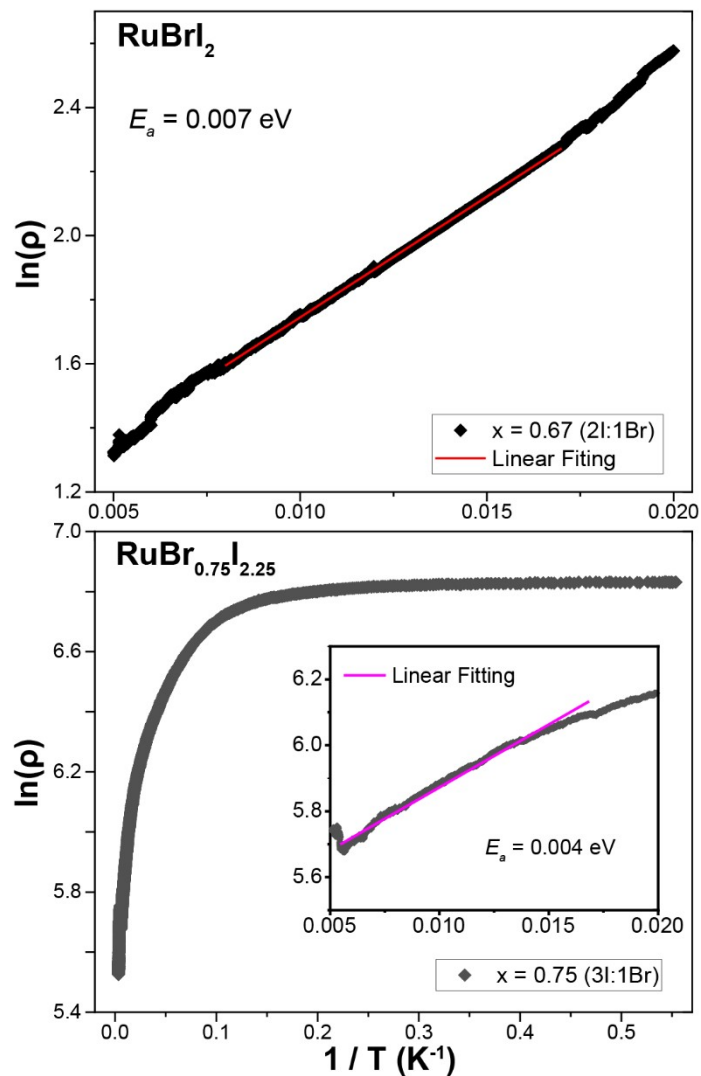


Figure S8. The plots of $\ln(\rho)$ vs $1/T$ of RuBr_2 (top) and $\text{RuBr}_{0.75}\text{I}_{2.25}$ (bottom) samples. Linear fitting of a high temperature range is conducted to calculate the activation energy. The nonlinear shape of $\text{RuBr}_{0.75}\text{I}_{2.25}$ sample's plot suggests an increased metallic component with higher iodine content in this sample.